The 2022 World Congress on
Advances in Civil, Environmental, & Materials Research (ACEM22)
16-19, August, 2022, GECE, Seoul, Korea

A framework for wind-induced vulnerability assessment of low-rise light steel buildings

*Zhou Haojie[1)], Wu Fengbo[2)], Huang Guoqing[3)]

[1), 3)] *School of Civil Engineering, Chongqing University, Chongqing, China*
[2)] *School of Civil Engineering, Chongqing Jiaotong University, Chongqing, China*
[2)] *fwu0923@cqjtu.edu.cn*

ABSTRACT

Low-rise light steel buildings are typical wind-sensitive structures, which suffered severe damage frequently during wind hazards. Based on stochastic simulation technology, a framework for the overall wind-induced vulnerability assessment of low-rise light steel buildings is developed in this paper. Firstly, the wind load randomization method is determined by referring to the ASCE Standard. Then, considering the uncertainty of materials and geometric properties, the fragility indicator of the main structure is obtained by nonlinear analysis of the finite element models. The wind-induced fragility of the envelope structure is analyzed with consideration of windborne debris and wind pressure. Furthermore, the loss ratio under different damage levels is capable to be calculated according to the structural construction cost. A specific numerical case is adopted to illustrate the proposed framework, it demonstrates that the method can integrate the wind-induced loss of the main structure and the envelope structure to obtain the overall vulnerability curve. Consequently, the economic loss of the low-rise light steel buildings can be quantified and it provides a basis for the determination of insurance premium rates.

1. INTRODUCTION

Numerous post-disaster surveys have revealed that the envelope structure of low-rise light steel buildings is severely damaged and the main structure may also collapse under strong winds (Yang et al. 2018), which highlights the necessity for wind-induced fragility and vulnerability assessment. Wind-induced fragility represents the probability of a structure/member that reaches or exceeds a certain damage state under different wind speeds, whereas wind-induced vulnerability represents a quantitative value of economic loss calculated by the wind-induced fragility indicator and construction cost.

[1)] Graduate Student
[2)] Lecturer
[3)] Professor

Many scholars have conducted research on the wind-induced fragility of low-rise light steel buildings in recent years. (Stewart et al. 2016) conducted a wind-induced fragility assessment of low-rise light steel buildings in Australia, and provided an approach to calculating load redistribution behavior and wind-induced internal pressure at roofing system connections. (Konthesingh et al. 2015) developed a model for estimating the loss of metal roof systems of industrial buildings in tropical cyclone-prone areas by considering the correlation between failure mechanisms and load-sharing behavior. Based on the simplified progressive damage process, (Wu et al. 2021) proposed a method to analyze the fragility of low-rise building envelopes by taking the effects of opening conditions, internal pressure variation, wind velocity/direction variability, and other factors into consideration systematically.

The above studies have mainly estimated the loss of the envelope structure, while less research has been conducted on the fragility of the main structure, resulting in the lack of a comprehensive analysis of the overall fragility and vulnerability. In this paper, a framework for the wind-induced vulnerability assessment of low-rise light steel buildings is proposed, based on which the damage to the main structure and the envelope structure caused by the combined effect of windborne debris and wind pressure, variability of wind load, and internal pressure variation can be better considered, and by extension, the economic indicator of wind-induced damage can be quantified.

2. WIND-INDUCED FRAGILITY ASSESSMENT

2.1 Wind load uncertainty analysis

The randomness of the wind load should be considered in the wind-induced fragility analysis. The American load standard(ASCE 2016) has conducted relatively sufficient research on this issue, so the paper refers to the ASCE 7-16 for the wind-induced fragility analysis of low-rise light steel buildings.

The wind loads on the main structure and envelope structure of enclosed/partially enclosed low-rise buildings can be calculated by Eq. (1):

$$p = q_h\left[\left(GC_{pf}\right)-\left(GC_{pi}\right)\right]$$
$$q_h = 0.613K_zK_{zt}K_dV^2 \quad (1)$$

where p is the design wind load; q_h is velocity pressure evaluated at mean roof height; GC_{pf} and GC_{pi} are the external and internal pressure coefficients respectively; G is the gust factor; K_z is the velocity pressure exposure coefficient; K_{zt} is the topography factor; K_d is the wind directionality factor; V is the basic wind speed. The parameters in Eq.(1) can be determined according to Ellingwood and Tekie (1999) and ASCE 7-16 (2016). It is worth noting that Eq.(1) cannot be used directly in the wind-induced fragility analysis of the main structure because the coefficients are obtained by considering the envelope values of wind pressure coefficients for each wind direction and have been multiplied by the reduction factor. Therefore, the wind direction reduction factor used for design should be ignored and GC_{pf} should be determined according to the wind pressure coefficient in each wind

direction.

Although the value of GC_{pi} is clearly defined by ASCE 7-16, for buildings with openings, the correlation between the internal and external pressure cannot be ignored. To make the simulations in the fragility analysis more closely match the damage process of the practical buildings, the calculation of the internal pressure coefficient can be carried out using the following equation(Stewart et al. 2016):

$$GC_{pi} = \frac{\sum_{k=1}^{K} A_{ok} GC_{pk}}{\sum_{k=1}^{K} A_{ok}} \tag{2}$$

where K is the number of openings in the envelope; A_{ok} is the area of the kth opening; GC_{pk} is the external pressure coefficient at the kth opening.

It can be seen that the internal pressure of the building depends on the opening condition. Mostly occurring on windward surfaces, openings are mainly caused by excessive wind pressure or windborne debris. The impact fracture probability of a single door or window caused by windborne debris can be expressed as(Cope 2004):

$$P_d = 1 - \exp\left(-n_c \times c_1 \times c_2 \times c_3 \times c_4\right) \tag{3}$$

where n_c denotes the total number of available missile objects converting from windborne debris; c_1 denotes the proportion of potential missile objects; c_2 denotes the number of missile objects that hit the house; c_3 denotes the ratio of the area of the window/door to the area of the wall on which the window/door is located; c_4 denotes the probability of the impact momentum of missile objects exceeding the threshold. The values of the parameters mentioned above are recommended to be used after the calibration in conjunction with the referenced standard, field research on the source of missile objects, sizes and materials of windows or doors, and protective measures.

2.2 Analysis of wind-induced fragility of the main structure

Under strong wind load, the rigid frame of low-rise light steel buildings may collapse due to excessive displacement or local buckling. With reference to the fragility analysis method of seismic engineering (Zhou et al. 2011), the process of wind-induced fragility of the main structure is divided into three steps: establishment of the uncertainty simulation models, nonlinear static analysis, and fitting fragility curve. Since the light steel buildings generally have more columns in the longitudinal direction and are equipped with braces, this paper addresses on the analysis of the transversal rigid frame. Fig. 1 is a schematic diagram of an uncertainty simulation model.

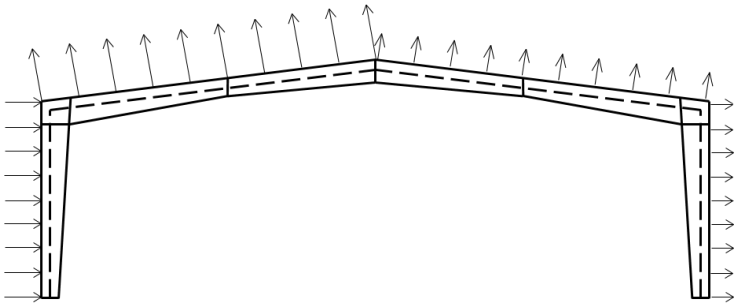

Fig.1 Schematic diagram of an uncertainty simulation model

Firstly, the finite element models of single-bay rigid frames are generated in batch based on the uncertainty of materials and geometric dimensions; secondly, the dead load and wind load generated by tentative wind speed are applied to the model, then the nonlinear static analysis is performed for each structure. By increasing the tentative wind speed and repeating the steps above, the number of structures exceeding the specific damage state under different wind speeds can be obtained. Taking the limit state of structural bearing capacity as the critical state, when the calculation process does not converge, the increment of tentative wind speed is automatically halved and the calculation continues to be solved. If the calculation still does not converge after several successive halvings, the structure is considered to have exceeded the specified limit state due to excessive deformation, and the wind speed at this time is the ultimate bearing capacity that makes the structure exceed the specified damage state. Finally, the ratio of the number of damaged structures to the total number of structures is the probability of exceeding the specified damage state, and the lognormal probability distribution is used to fit these probability values to obtain the wind-induced fragility curve of the main structure.

2.3 Analysis of wind-induced fragility of the envelope structure

The most vulnerable components of the envelope structure during wind hazards are windows, doors, and roof panels. Hence, the failure of windows, doors, and roof panels in low-rise light steel buildings are selected emphatically for illustration in this section.

2.3.1 Doors and windows

Windborne debris or excessive wind pressure can lead to damage to doors and windows of low-rise buildings. Due to a lack of mature research and sufficient data, the correlation between the effect of wind pressure and the impact of windborne debris is excluded hereinafter. The failure probability of an individual door or window can be expressed by the following equation:

$$P_{wd} = P_w + P_d - P_w P_d \tag{4}$$

where P_{wd} denotes the failure probability of an individual door or window; P_d denotes the probability of a window or door broken due to windborne debris' impact; P_w denotes the failure probability caused by excessive wind pressure. Generally speaking, W and R are two mutually independent random variables. P_d can be calculated according to Eq.(3), while P_w can be expressed as:

$$P_w = \iint_{r \le w} f_W(w) f_R(r) dr dw \tag{5}$$

where $f_W(w)$ is the probability density function of wind-induced response extremes; $f_R(r)$ is the probability density function of bearing capacity of wind pressure.

Supposing that the number of windows and doors is *M*. Let the indicator vector Q_i denotes the damage condition of *i*th window or door, where Q_i=1 or 0 denotes a damaged or intact window/door, respectively. The damage ratio defined as the percentage of failed components is regularly used to describe the losses on envelope structure, and damage ratio of windows/doors is written accordingly:

$$D_W = M^{-1} \sum_{i=1}^{M} Q_i \tag{6}$$

2.3.2 Roof panels

Once the doors or windows are damaged, the building becomes a structure with openings and its internal pressure should be recalculated. To obtain the net wind load on the roof panel, the internal pressure is calculated according to Eq.(2) based on the simulated external pressure, thereby the net wind pressure to which the roof panel is subjected can be determined. And the internal forces of screws can be obtained based on the continuous beam assumption (Henderson and Ginger 2011).

It has been revealed that when a screw fails, the load it carried before failure is to redistribute, and about 90% of this load is distributed to two adjacent screws on the same crest. The internal forces of these adjacent screws increase sharply, causing these screws to fail one after another as well consequently(Ji et al. 2018). It can be considered that the whole panel is damaged after any screw on the roof panel fails, and then the failure probability of the roof panel can be expressed as:

$$p = 1 - \iint_{w_1 < r_1} \iint_{w_2 < r_2} \cdots \iint_{w_{n_s} < r_{n_s}} f_{\mathbf{R}}(\mathbf{r}) f_{\mathbf{W}}(\mathbf{w}) d\mathbf{r} d\mathbf{w} \tag{7}$$

where f_R (r) denotes the joint distribution of the strength roof panel; f_W (w) denotes the joint distribution of internal forces at each screw; n_s denotes the number of screws on a roof panel.

Assume that the number of roof panels is *N*. Let B_n denote the indicator vector of the *n*th roof panel, where B_n =1 or 0 denotes a damaged or intact panel, respectively. Then the damage ratio of panels can be expressed as follows:

$$D_R = N^{-1} \sum_{n=1}^{N} B_n \tag{8}$$

2.4 Overall wind-induced fragility analysis

The aforementioned section conducts wind-induced fragility analysis for the main structure and the envelope structure. Whereas, the insurance industry is more interested in the overall wind-induced economic losses of low-rise light steel buildings. This paper

focuses on the correlation between the wind loads on the main structure, windows, doors, and roofing system in the progressive failure process. Based on this, the framework for the overall wind-induced vulnerability analysis of the low-rise light steel buildings is shown in Fig.2.

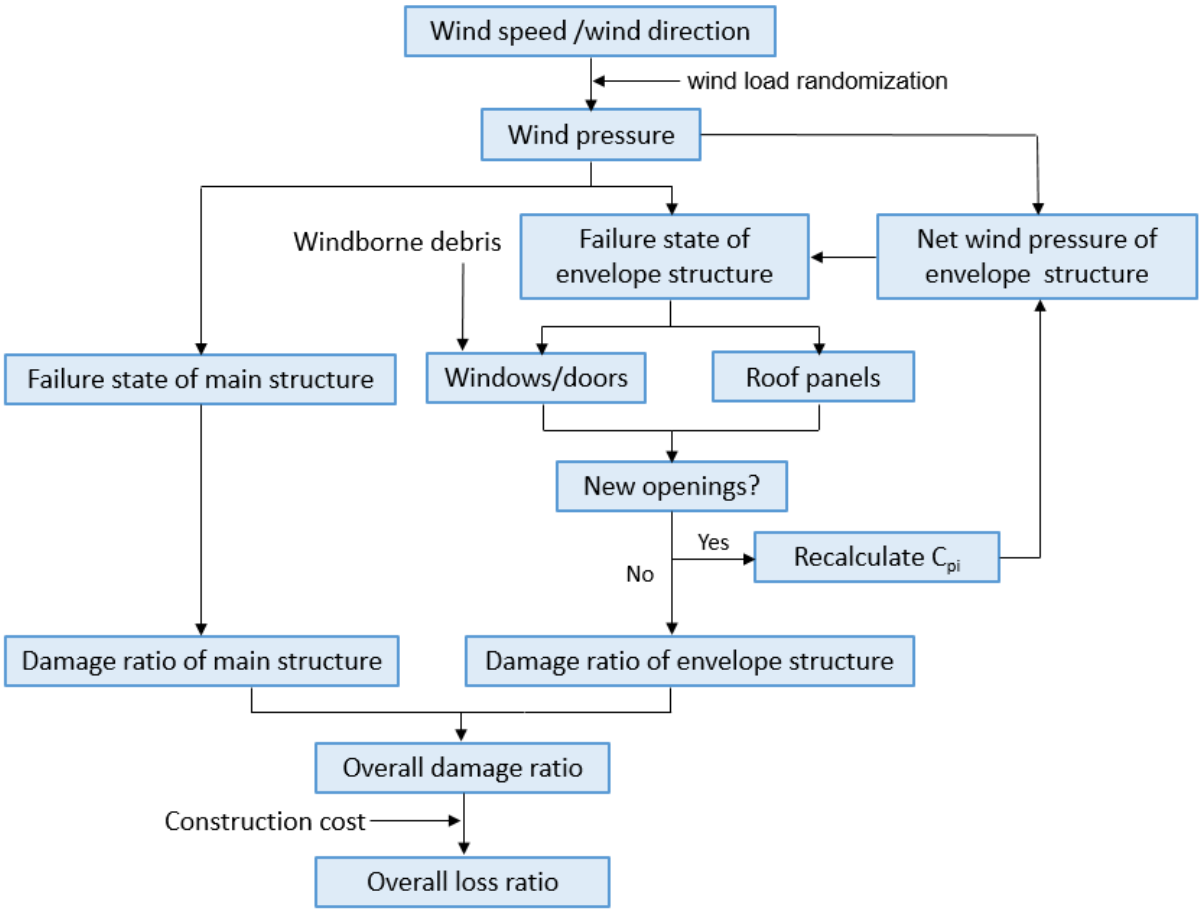

Fig.2 Framework for the overall wind-induced vulnerability assessment of low-rise light steel buildings

For a low-rise light steel building with M bay rigid frames, W windows/doors, and N roof panels, Monte Carlo simulations (MCS) are used in this paper to analyze its wind-induced fragility at specified wind speeds and directions. In the MCS-based approach, a total of N_c=5000 simulation rounds are employed, where the lth (l=1,2..., N_c) simulation is performed according to the following steps:

(1) Based on the probability distributions of the parameters mentioned in section 2.1 and Eq.(1), stochastic simulations can be performed to obtain wind load samples Y_M for the main structure, Y_W for the windows and doors, and Y_R for the roof panels, respectively.

(2) For the main structure, based on the probabilistic model of materials and geometric dimensions, a set of single-bay rigid frames can be randomly simulated, and nonlinear static analysis is performed for each of them to determine whether each bay collapses. The collapse state of the *i*th *rigid* frame in the *l*th simulation is given by $H_{i,l}$. If it collapses, $H_{i,l}$= 1, otherwise $H_{i,l}$= 0, and calculate the damage ratio of the main structure in this simulation: $D_{M,l} = \frac{1}{M}\sum_{i=1}^{M} H_{i,l}$.

(3) For the envelope structure, the following methods are used to consider the progressive destruction.

①For windows and doors, the failure probability P_w of windows and doors under wind pressure is calculated based on Y_W , and the failure probability of windows and doors under the impact of windborne debris P_d is calculated based on wind speed according to Eq.(3), and then the failure probability P_i of each window or door is determined by Eq.(4); meanwhile, random numbers A_i are obtained by using random simulation. Denote $Q_{i,l}$ as the failure state of the *i*th window or door in the *l*th simulation. If $A_i < P_i$, *the i*th *window or door fails in* this simulation, $Q_{i,l}$=1, otherwise $Q_{i,l}$=0.

②For the roof panel, simulate a set of roof panel bearing capacity samples *R*. Compare the numerical value of Y_R and *R* to determine whether the panel fails. $B_{i,l}$ is used to indicate the failure state of the *i*th *panel* in this simulation. If it fails, $B_{i,l}$ =1, otherwise $B_{i,l}$=0.

③If the building does not have new openings, calculate the damage ratio of windows and doors in this simulation: $D_{W,l} = W^{-1}\sum_{i=1}^{W} Q_{i,l}$, and the damage ratio of roofs: $D_{R,l} = N^{-1}\sum_{i=1}^{N} B_{i,l}$; if the building has new openings, recalculate the internal pressure according to Eq.(2) and substitute it into Eq.(1) and Eq.(4) to redetermine the failure probability P_i for the remaining windows and doors that have not yet failed and the wind load Y_R for the roof panels. Compare the numerical value of P_i and A_i to determine the failure state of the remaining windows and doors. If the *i*th window or door failed, record $Q_{i,l}$ =1. Meanwhile, compare the numerical value of Y_R and *R to* determine the failure state of the remaining roof panels. If the *i*th panel failed, record $B_{i,l}$ =1. Finally, calculate the damage ratio of windows/doors: $D_{W,l} = W^{-1}\sum_{i=1}^{W} Q_{i,l}$ and the damage ratio of roofs: $D_{R,l} = N^{-1}\sum_{i=1}^{N} B_{i,l}$ in this simulation.

(4) Repeat steps (1) to steps (3) for a total of N_c times to extract and record the results of each simulation. Referring to the classification criterion adopted for HAZUS-MH hazard model, the damage state of all the above simulations is classified according to Table 1. Record the number of structures reaching or exceeding each damage level, divided by N_c to obtain the fragility indicator.

Table 1 Classification of damage levels for low-rise light steel buildings

Damage level	Grading	Main structure damage D_M	Envelope structure	
			Roof damage D_R	Window/door damage D_W
I	No damage	0 bays	$D_R \leq 2\%$	0 pcs
II	Minor damage	0 bays	$2\% < D_R \leq 15\%$	1 pcs
III	Moderate damage	0 bays	$15\% < D_R \leq 50\%$	> 1 pcs & < 3pcs / $D_W \leq 20\%$
IV	Serious damage	$D_M \leq 50\%$	$D_R > 50\%$	$20\% < D_W$ / 3 pcs & $D_W \leq 50\%$
V	Total destruction	$D_M > 50\%$	$D_R > 50\%$	$D_W > 50\%$

3. THE OVERALL WIND-INDUCED VULNERABILITY ASSESSMENT OF LOW-RISE LIGHT STEEL BUILDINGS

As described in section 2.4, a total of N_c simulations are performed, and the results of each simulation were extracted and recorded: the damage ratio of the main structure $D_{M,l}$, the damage ratio of the roof panels $D_{R,l}$, and the damage ratio of the windows/doors $D_{W,l}$ (l=1,2,..., N_c). All simulation results are now classified, and the same classes are grouped together in one category, as shown in Table 2.

Define the loss ratio L for low-rise light steel buildings as:

$$L = R_c / C_c \tag{9}$$

where C_c is the construction cost, which is equal to the sum of the cost of the structure, foundation, renovation, plumbing, HVAC, and taxes.; R_c is the cost of repair, which can be expressed as:

$$R_c = \sum_{i=1}^{K} Q_i D_i + C_p \tag{10}$$

where Q_i is the total price of the ith (i=1,2,...,K) component, which can be calculated by unit price and the total number of components, where K is the total number of component categories; D_i is the damage ratio of the ith component; C_p is the labor cost.

Substituting the total price and the damage ratios of components (Table 2) into Eq. (9), the repair costs corresponding to each loss rate sample in different damage classes can be calculated, and then combined with the overall cost of the building, the loss ratio corresponding to each loss rate sample in the specified damage class can be calculated based on Eq.(10), for example, the jth damage ratio sample in class I (j=1,2,...,N_I) loss ratio samples L_j^I is as follow:

$$L_j^I = Q_M D_{M,j}^I + Q_R D_{R,j}^I + Q_W D_{W,j}^I \tag{11}$$

where Q_M , Q_R, and Q_W denote the total price of main structure components, roof panels, and window/door components, respectively; $D^I_{M,j}$, $D^I_{R,j}$, and $D^I_{W,j}$ denote the *j*th damage ratio sample corresponding to the main structure, roof panels, and window/door components respectively in grade *I*.

Table 2 Categorization of damage levels

Damage level	Components Destruction { D_M , D_R , D_W }
I	$\{D^{I}_{M,1},D^{I}_{R,1},D^{I}_{W,1}\}, \{D^{I}_{M,2},D^{I}_{R,2},D^{I}_{W,2}\},\cdots, \{D^{I}_{M,N_I},D^{I}_{R,N_I},D^{I}_{W,N_I}\}$
II	$\{D^{II}_{M,N_I+1},D^{II}_{R,N_I+1},D^{II}_{W,N_I+1}\}, \{D^{II}_{M,N_I+2},D^{II}_{R,N_I+2},D^{II}_{W,N_I+2}\},\cdots, \{D^{II}_{M,N_{II}},D^{II}_{R,N_{II}},D^{II}_{W,N_{II}}\}$
III	$\{D^{III}_{M,N_{II}+1},D^{III}_{R,N_{II}+1},D^{III}_{W,N_{II}+1}\}, \{D^{III}_{M,N_{II}+2},D^{III}_{R,N_{II}+2},D^{III}_{W,N_{II}+2}\},\cdots, \{D^{III}_{M,N_{III}},D^{III}_{R,N_{III}},D^{III}_{W,N_{III}}\}$
IV	$\{D^{IV}_{M,N_{III}+1},D^{IV}_{R,N_{III}+1},D^{IV}_{W,N_{III}+1}\}, \{D^{IV}_{M,N_{III}+2},D^{IV}_{R,N_{III}+2},D^{IV}_{W,N_{III}+2}\},\cdots, \{D^{IV}_{M,N_{IV}},D^{IV}_{R,N_{IV}},D^{IV}_{W,N_{IV}}\}$
V	$\{D^{V}_{M,N_{IV}+1},D^{V}_{R,N_{IV}+1},D^{V}_{W,N_{IV}+1}\}, \{D^{V}_{M,N_{IV}+2},D^{V}_{R,N_{IV}+2},D^{V}_{W,N_{IV}+2}\},\cdots, \{D^{V}_{M,N_V},D^{V}_{R,N_V},D^{V}_{W,N_V}\}$

Note: $N_I + N_{II} + N_{III} + N_{IV} + N_V = N_C$

After a total of *Nc*=5000 simulation rounds employed, based on samples at the specified damage level (e.g., loss ratio samples in level *I* : $L^I_1, L^I_2, \ldots, L^I_{N_I}$), the statistical value of the loss ratio under specified damage level can be obtained.

4. NUMERICAL CASE STUDY

4.1 building prototype

As shown in Fig.3, a single-story low-rise light steel industrial building is used to illustrate the proposed framework. The building dimensions are 24.4 m in width, 38.1 m in length, and 8.631 m in height with the gable roof rising from an eave height of 7.615 m at a slope of 1/12. The beams and columns are all made of Q345 steel with I-cross sections .

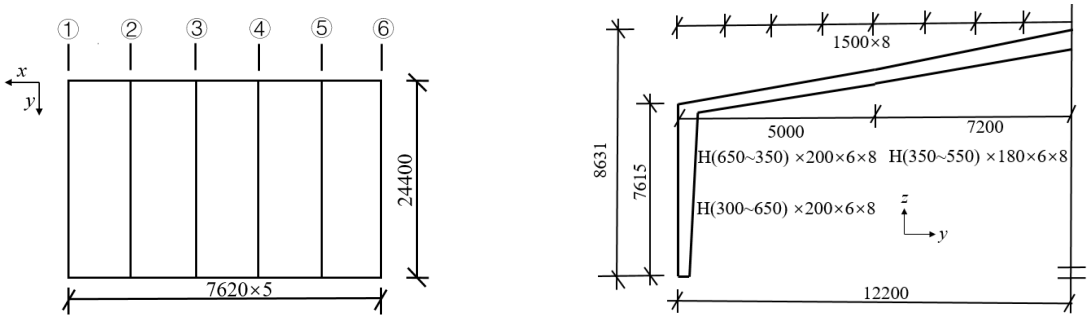

(a) (b)

Fig.3 Schematic diagram layout of portal frame
(a) Plan view of portal frame layout; (b) Single-bay portal frame sections

The schematic diagram of the envelope structure is shown in Fig.4(a). In addition, one door and two windows are arranged for each hill wall, and two doors and four windows are arranged for each longitudinal wall. The panels are made of YX35-125-750 medium wave trapezoidal profile sheets with the thickness of 0.6 mm, wave height of 35 mm, and adjacent wave spacing of 125 mm, as shown in Fig.4(b). Self-drilling screws are selected as the connecting elements between the panels and purlins/grits, with one screw set at each crest interval. The purlins and grits are arranged to be evenly spaced 2.0m and 1.5 m along the roof and wall respectively.

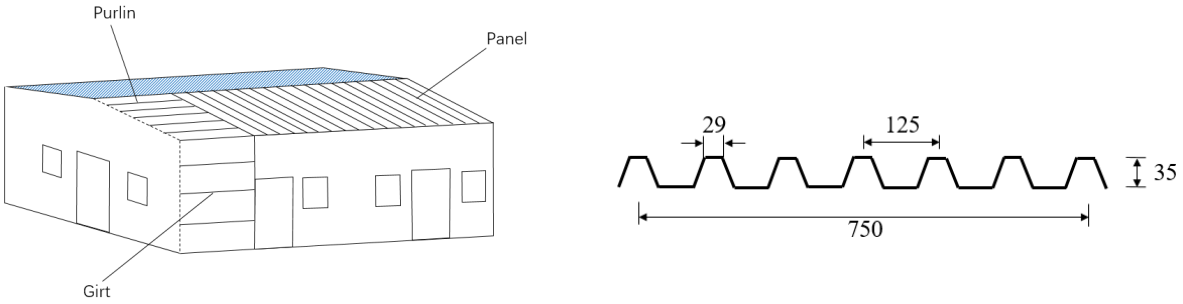

Fig.4 Schematic diagram of the envelope structure
(a) envelope structure layout; (b) cross-section of trapezoidal profile sheet

The main variable parameters of the I-cross sections include modulus of elasticity, Poisson's ratio, density, yield strength, etc. In this paper, the probability distributions of the relevant material parameters and the values of the parameters taken are shown in Table 3 (Lei et al. 2018).

Table 3 Probability distribution of material parameters

Random Variables	Nominal value	Cov	Distribution
Modulus of elasticity	2.06×10^6 MPa	0.03	Log-normal
Poisson's ratio	0.3	0.03	Log-normal
Density	7800 kg/m^3	-	Constant
Yield strength of Q235 steel	263.7 MPa	0.07	Log-normal
Yield strength of Q345 steel	387.1 MPa	0.07	Log-normal

The geometric dimensions of I-cross section members are inevitably affected by external factors during fabrication, transportation, and installation, thus the geometric dimensions are uncertain. It is suggested that the probability distribution of the geometric dimensions subjects to a normal distribution, and the statistical parameters of the sections are shown in Table 4(Li et al. 2010).

Table 4 Probability distribution of geometric dimensions

Cross-section dimensions	Actual mean value /standard value	Cov	Distribution
Web thickness	0.981	0.034	Normal
Flange *width*	1.005	0.011	Normal
Cross-section height	1.003	0.011	Normal
Steel plate thickness	0.979	0.022	Normal

4.2 Results of numerical case

In this paper, SAP2000 software is used to establish the finite element models for the rigid frames, as shown in Fig. 5. The stress-strain relationship of the steel is taken as ideal elastoplasticity. To perform nonlinear analysis, FEMA-356 plastic hinges are set at 0.1 times and 0.9 times the distance from the beam end and column end.

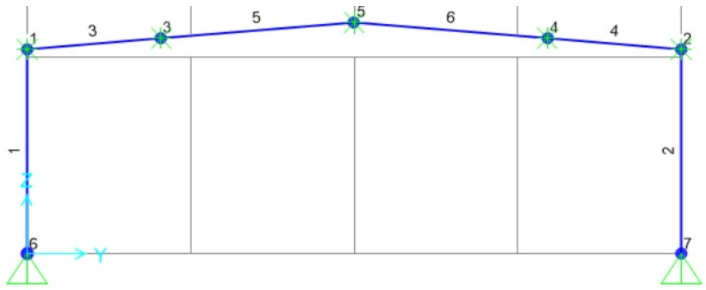

Fig.5 Finite element model of a rigid frame

Considering the uncertainty of material parameters and geometric dimensions, 500 structures are generated. The results of the analysis above are shown in Fig.6(a). It can be noted that when the building is under lower wind speed (less than 20 m/s), the light steel structure is slightly damaged; for higher wind speed (higher than 35 m/s), the structure has a higher probability of severe damage, while the probability of overall destruction is still small; when the wind speed reaches 50 m/s, the whole structure almost collapses completely.

It is assumed that the bearing capacity of glass windows and doors subjects to a normal distribution with a mean value of 5 kN/m^2 and a Cov of 0.2 (Wu et al., 2021), and the damage ratios of windows and doors are obtained according to the procedure described in section 1.4. For the integration with the main structure analysis, the total number of simulations is taken as N_c = 500. When the number of random simulations required is higher (e.g., N_c = 5000), the non-parametric method “bootstrap”(Naess and Clausen 2001) can be used to extend the sample of the main structure considering the non-linear analysis of the main structure is time-consuming.

Fig.6(b) displays the mean and standard deviation of the damage ratio of the doors and windows(D_W) at different wind speeds. It can be seen that the doors and windows go breaking gradually when wind speeds are greater than 30 m/s, and the standard deviation of loss ratio reaches the maximum value at a wind speed of 38 m/s.

Random simulations are performed for the specified wind speed, and the damage ratio of roof panels(D_R) is obtained by Eq.(8). The mean and standard deviation of the damage ratio are given in Fig.6(c). It can be seen that the mean value and standard deviation of the damage ratio of roof panels are almost zero when the wind speed is relatively small (V<40m/s), and it starts to ascend gradually when wind speed is greater than 40m/s, and the standard deviation reaches the maximum value at the wind speed of 58m/s.

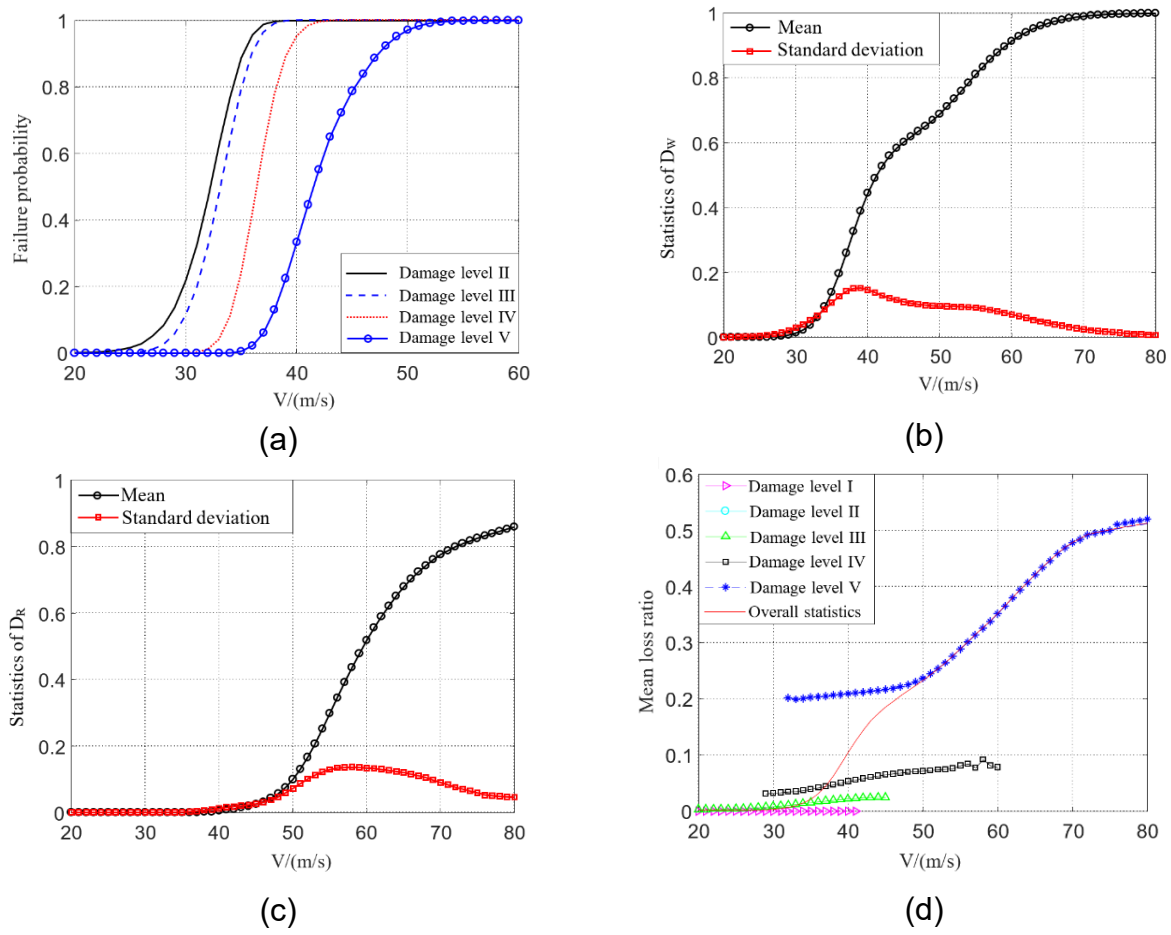

Fig.6 The results of numerical case study

Based on the level classification method proposed in section 1.4, the mean values of loss ratios for different damage levels at different wind speeds are given in Fig.6(d), where the overall statistics indicate mean values of loss ratios corresponding to all N_c times simulated damage results without classification. It can be noted that with the increase of wind speed, the loss ratio elevates gradually, and the loss ratio of the overall statistics tends to be consistent with the loss ratio under damage level V. The overall statistics mean loss ratio is comparatively small at low wind speed.

5. CONCLUSION

Based on Monte Carlo simulation, the paper proposed a wind-induced vulnerability assessment framework for low-rise light steel buildings, based on which the combined effect of windborne debris and wind pressure, wind load variability, and internal pressure variation can be better considered. The following conclusions can be drawn from the numerical case study.

(1) The framework is capable of considering the damage to vulnerable elements on windward surfaces under the combined action of windborne debris and wind pressure.

(2) The effect of internal pressure variations on roof panel losses during complex progressive damage of low-rise light steel buildings is analyzed in a simplified and effective approach.

(3) Based on this framework, the wind-induced fragility of the main structure and the envelope structure can be better integrated, consequently, the damage state of the low-rise light steel buildings under the specified wind speed can be more systematically and comprehensively evaluated, and the overall vulnerability curve can be obtained. Furthermore, the wind-induced losses can be quantified to satisfy the demand for wind hazard mitigation and risk management.

REFERENCES

American Society of Civil Engineers (ASCE).(2016), “Minimum design loads for buildings and other structures. *ASCE standard 7-16*”, Reston, Va.

Cope, A.D. (2004), “Predicting the vulnerability of typical residential buildings to hurricane damage”. *Florida: University of Florida. Department of Civil and Coastal Engineering*, 70.

Ellingwood, B.R, Tekie, P.B. (1999), “Wind load statistics for probability-based structural design”, *J. Struct. Eng.* , 125 (4): 453-463.

Ji, X.W., Huang, G.Q., Zhang, X.X., Kopp, G.A. (2018), “Vulnerability analysis of steel roofing cladding: Influence of wind directionality”, *Eng. Struct.* , 156: 587-597.

Konthesingha, K.C., Stewart, M.G., Ryan, P., Ginger, J., & Henderson, D. (2015), “Reliability-based vulnerability modelling of metal-clad industrial buildings to extreme wind loading for cyclonic regions”, *J. Wind. Wind. Eng. Ind. Aerodyn.*, 147, 176-185.

Lei, X., Fu, X., Xiao, K., Wang, J., Nie, M., Li, H.N., Xie, W.P. (2018), “Failure Analysis of a Transmission Tower Subjected to Wind Load Using Uncertainty Method”, *Proceedings of the CSEE*, 38(S1):266-274. (in Chinese)

Li, K., Liu, Z.J., Sun, K.C. (2010), “Calibration analysis of reliability of steel highway bridges in China”, *Eng. J. Wuhan Univ.*, 43(04):499-506. (in Chinese)

Naess, A., Clausen, P.H. (2001), “Combination of the peaks-over-threshold and bootstrapping methods for extreme value prediction”, *Struct. Saf.*, 23(4): 315-330.

Stewart, M.G., Ryan, P.C., Henderson, D.J., Ginger, J.D. (2016), “Fragility analysis of roof damage to industrial buildings subject to extreme wind loading in non-cyclonic regions”, *Eng. Struct.,* 128: 333-343.

Vickery, P.J., Skerlj, P.F., Lin, J., Twisdale, L.A., Young, M.A., Lavelle, F.M. (2006), “HAZUS-MH hurricane model methodology II: Damage and loss estimation”, *Nat. Hazards Rev.*, 7(2): 94-103.

Wu, F.B., JI, X.W., Huang, G.Q., Zhao, Y.G. (2021), “Wind-induced fragility analysis of low-rise building envelope based on simplified progressive damage”, *J. Build. Struct.* 2021, 42(05): 32-39. (in Chinese)

Yang, Q.S., Gao, R., Bai, F., Li, T., Tamura, Y. (2018), “Damage to buildings and structures due to recent devastating wind hazards in East Asia”, *Nat. Hazards,* 2018, 92(3): 1321-1353.

Zhao, M.W., Gu, M. (2012), “Probabilistic wind vulnerability analysis of light-weight steel buildings”, *J. S.-Cent. Univ. Natl. (Nat. Sci. Ed.)*, 43(09): 3609-3618. (in Chinese)
Zhou, K., Li, W., Yu, J.X. (2011), “Review of seismic fragility analysis methods”. *Earthq. Eng. Eng. Vib.*, 31(01):106-113. (in Chinese)